

Overcritical Rotation of a Trapped Bose-Einstein Condensate

A. Recati^a, F. Zambelli^b, and S. Stringari^b

^a*International School of Advanced Studies, Via Beirut 2/4, I-34014 Trieste, Italy*

^b*Dipartimento di Fisica, Università di Trento,*

and Istituto Nazionale per la Fisica della Materia, I-38050 Povo, Italy

(May 3, 2019)

The rotational motion of an interacting Bose-Einstein condensate confined by a harmonic trap is investigated by solving the hydrodynamic equations of superfluids, with the irrotationality constraint for the velocity field. We point out the occurrence of an overcritical branch where the system can rotate with angular velocity larger than the oscillator frequencies. We show that in the case of isotropic trapping the system exhibits a bifurcation from an axisymmetric to a triaxial configuration, as a consequence of the interatomic forces. The dynamical stability of the rotational motion with respect to the dipole and quadrupole oscillations is explicitly discussed.

PACS numbers: 03.75.Fi, 05.30.Jp, 32.80.Pj, 67.40.-w

An important peculiarity of harmonic trapping is the existence of a critical angular velocity, fixed by the oscillator frequencies, above which no system can rotate in conditions of thermal equilibrium. The main purpose of this work is to show that a trapped Bose-Einstein condensate at very low temperature can rotate at angular velocities higher than the oscillator frequencies in a regime of dynamical equilibrium. The occurrence of overcritical rotations is a rather well established feature in classical mechanics (see, for example, [1,2]) and is the result of the crucial role played by the Coriolis force. It is therefore interesting to understand the new features exhibited by rotating superfluids and in particular the role played by Bose-Einstein condensation. The rotational behaviour of superfluids is, in fact, deeply influenced by the constraint of irrotationality which makes it impossible, for such systems, to rotate in a rigid way. Spectacular consequences of irrotationality are the quenching of the moment of inertia with respect to the rigid value and the occurrence of quantized vortices [3]. Both these effects have been recently observed in dilute gases confined in harmonic traps [4–6].

We start our analysis by considering a dilute Bose gas interacting with repulsive forces at zero temperature. For large systems, where the Thomas-Fermi approximation applies, the equations of motion are well described by the so called hydrodynamic theory of superfluids [7,8]. If the confining potential rotates with angular velocity Ω it is convenient to write these equations in the frame rotating with the angular velocity of the trap, where they take the form:

$$\frac{\partial \rho}{\partial t} + \nabla \cdot (\rho(\mathbf{v} - \boldsymbol{\Omega} \times \mathbf{r})) = 0 \quad (1)$$

$$\frac{\partial \mathbf{v}}{\partial t} + \nabla \cdot \left(\frac{v^2}{2} + \frac{V_{\text{ext}}(\mathbf{r})}{M} + \frac{\mu_{\text{loc}}(\rho)}{M} - \mathbf{v} \cdot (\boldsymbol{\Omega} \times \mathbf{r}) \right) = 0. \quad (2)$$

In the above equations $V_{\text{ext}}(\mathbf{r}) = M(\omega_x^2 x^2 + \omega_y^2 y^2 + \omega_z^2 z^2)/2$ is the oscillator potential providing the external confinement. Notice that in the rotating frame $V_{\text{ext}}(\mathbf{r})$ does not depend on time. Furthermore $\mu_{\text{loc}}(\rho) = g\rho$ is the chemical potential of the uniform gas, where $g = 4\pi\hbar^2 a/M$ is the coupling constant fixed by the s -wave scattering length a and \mathbf{v} is the velocity field in the laboratory frame, expressed in terms of the coordinates in the rotating frame. It satisfies the irrotationality constraint. Eqs. (1)-(2) can be applied also to a trapped Fermi superfluid where the expression for $\mu_{\text{loc}}(\rho)$ takes, of course, a different form. The stationary solutions in the rotating frame are obtained by imposing the conditions $\partial\rho/\partial t = 0$ and $\partial\mathbf{v}/\partial t = 0$. Let us look for solutions of the form [9]

$$\mathbf{v} = \alpha \nabla(xy) \quad (3)$$

for the velocity field, where α is a parameter that will be determined later. Choice (3) for the velocity field rules out the description of vortical configurations. Vortices cannot be in any case described by the hydrodynamic equations (1)-(2) since they require the use of more microscopic approaches, like Gross-Pitaevskii theory for the order parameter, accounting for the behaviour of the system at distances of the order of the healing length [10,8]. Since the critical frequency needed to generate a stable vortex becomes smaller and smaller as the number of atoms increases [11], the solutions discussed in the present work correspond, in general, to metastable configurations.

By substituting expression (3) into Eq. (2) one immediately finds that the resulting equilibrium density is given by the parabolic shape

$$\rho(\mathbf{r}) = \frac{1}{g} \left[\tilde{\mu} - \frac{M}{2} (\tilde{\omega}_x^2 x^2 + \tilde{\omega}_y^2 y^2 + \omega_z^2 z^2) \right] \quad (4)$$

also in the presence of the rotation. Of course Eq. (4) defines the density only in the region where $\rho > 0$. Elsewhere one should put $\rho = 0$. The new distribution is characterized by the effective oscillator frequencies

$$\tilde{\omega}_x^2 = \omega_x^2 + \alpha^2 - 2\alpha\Omega \quad (5)$$

$$\tilde{\omega}_y^2 = \omega_y^2 + \alpha^2 + 2\alpha\Omega, \quad (6)$$

which fix the average square radii of the atomic cloud through the relationships

$$\tilde{\omega}_x^2 \langle x^2 \rangle = \tilde{\omega}_y^2 \langle y^2 \rangle = \omega_z^2 \langle z^2 \rangle = \frac{2\tilde{\mu}}{7M}, \quad (7)$$

where the quantity

$$\tilde{\mu} = \frac{\hbar\tilde{\omega}_{ho}}{2} \left(\frac{15Na}{\tilde{a}_{ho}} \right)^{2/5} \quad (8)$$

is the chemical potential in the rotating frame and ensures the proper normalization of the density (4). In Eq. (8) we have defined $\tilde{\omega}_{ho} = (\tilde{\omega}_x\tilde{\omega}_y\omega_z)^{1/3}$ and $\tilde{a}_{ho} = \sqrt{\hbar/M\tilde{\omega}_{ho}}$. The applicability of the Thomas-Fermi approximation, and hence of the hydrodynamic equations (1)-(2), requires that the parameter $15Na/\tilde{a}_{ho}$ be much larger than unity. The rotation of the trap, providing a value of α different from zero, has the consequence of modifying the shape of the density profile, through the change of the effective frequencies $\tilde{\omega}_x$ and $\tilde{\omega}_y$. For certain values of Ω this effect can destabilize the system. Physically one should impose the conditions $\tilde{\omega}_x^2 > 0$, $\tilde{\omega}_y^2 > 0$ to ensure the normalizability of the density.

The equation of continuity (1), which at equilibrium takes the form $(\mathbf{v} - \boldsymbol{\Omega} \times \mathbf{r}) \cdot \nabla \rho(\mathbf{r}) = 0$, yields the following expression for α

$$\alpha = -\Omega \left(\frac{\tilde{\omega}_x^2 - \tilde{\omega}_y^2}{\tilde{\omega}_x^2 + \tilde{\omega}_y^2} \right) \quad (9)$$

in terms of Ω and of the effective frequencies $\tilde{\omega}_x, \tilde{\omega}_y$. From (9) and (7) one finds that the expectation value of the angular momentum

$$\langle L_z \rangle = M \int (\mathbf{r} \times \mathbf{v})_z n(\mathbf{r}) d\mathbf{r} \equiv \Omega\Theta \quad (10)$$

is always fixed by the irrotational value $\Theta = NM(\langle x^2 - y^2 \rangle)^2 / \langle x^2 + y^2 \rangle$ of the moment of inertia [12]. In terms of the effective frequencies $\tilde{\omega}_x$ and $\tilde{\omega}_y$ the ratio between Θ and the classical rigid value $\Theta_{\text{rig}} = NM\langle x^2 + y^2 \rangle$ takes the simple expression

$$\frac{\Theta}{\Theta_{\text{rig}}} = \left(\frac{\tilde{\omega}_x^2 - \tilde{\omega}_y^2}{\tilde{\omega}_x^2 + \tilde{\omega}_y^2} \right)^2. \quad (11)$$

Notice that both Θ and Θ_{rig} depend on the value of Ω since the square radii $\langle x^2 \rangle$ and $\langle y^2 \rangle$ are modified by the rotation.

Another useful quantity to calculate is the release energy $E_{\text{rel}} = E_{\text{kin}} + E_{\text{int}}$ giving the energy of the system after switching off the confining trap. This quantity can be extracted from time of flight measurements on the expanding cloud. In non rotating condensates it coincides with the interaction energy if one works in the Thomas-Fermi regime. In the presence of the rotation the kinetic energy $E_{\text{kin}} = M \int d\mathbf{r} n(\mathbf{r}) v^2/2$ cannot be instead neglected. By using the virial identity [8] $2E_{\text{kin}} - 2E_{\text{ho}} + 3E_{\text{int}} = 0$, where E_{ho} is the expectation value of the oscillator potential, and noting that $E_{\text{int}} = (2/7)N\tilde{\mu}$, one finds the result

$$\frac{E_{\text{rel}}}{N} = \frac{\tilde{\mu}}{7} \left(\frac{\omega_x^2}{\tilde{\omega}_x^2} + \frac{\omega_y^2}{\tilde{\omega}_y^2} \right). \quad (12)$$

Let us now discuss the explicit behaviour of the stationary solutions of the hydrodynamic equations (1)-(2). By inserting expressions (5) and (6) into Eq.(9) one finds the following third order equation for α [13]:

$$2\alpha^3 + \alpha(\omega_x^2 + \omega_y^2 - 4\Omega^2) + \Omega(\omega_x^2 - \omega_y^2) = 0. \quad (13)$$

Depending on the value of Ω and of the deformation

$$\epsilon = \frac{\omega_x^2 - \omega_y^2}{\omega_x^2 + \omega_y^2} \quad (14)$$

of the trap, one can find either 1 or 3 solutions, derivable in analytic form. As already anticipated, the physical solutions should satisfy the additional requirements $\tilde{\omega}_x^2 > 0$ and $\tilde{\omega}_y^2 > 0$, which ensure the normalizability of the density and rule out some of the solutions of (13). The resulting phase diagram is reported in Fig. 1 where, in the plane $\Omega - \epsilon$, we show explicitly the regions characterized by 0,1,2 and 3 solutions (we assume hereafter $\epsilon > 0$). The solid curve, given by

$$\frac{\epsilon^2 \Omega^2}{\omega_x^2 + \omega_y^2} + \frac{2}{27} \left(1 - 4 \frac{\Omega^2}{\omega_x^2 + \omega_y^2} \right)^3 = 0, \quad (15)$$

divides the plane in two parts: on the left hand side Eq. (13) admits only one solution, on the right hand side it has three solutions. The dotted lines are the curves $\Omega = \omega_y = \omega_x \sqrt{(1-\epsilon)/(1+\epsilon)}$ and $\Omega = \omega_x$. If $\epsilon < 0.2$ one can find (see Fig. 1) 3 stationary solutions, by properly choosing the value of Ω [14]. It is worth noticing that the phase diagram of Fig. 1 differs from the one derivable in the non-interacting Bose gas confined by the same harmonic trap. In this case the density profile in the rotating frame has the Gaussian shape $\rho(\mathbf{r}) = N (M\tilde{\omega}_{\text{ho}}/\pi\hbar)^{3/2} \exp[-M(\tilde{\omega}_x x^2 + \tilde{\omega}_y y^2 + \omega_z z^2)/\hbar]$. The renormalized frequencies still obey the Equations (5) and (6), but the relationship for α takes the different form $\alpha = -\Omega(\tilde{\omega}_x - \tilde{\omega}_y)/(\tilde{\omega}_x + \tilde{\omega}_y)$. In the non interacting case one finds that only one stationary solution is available for $\Omega < \omega_y$ and $\Omega > \omega_x$, while no solution exists in the interval $\omega_y < \Omega < \omega_x$.

In Figs. 2 and 3 we show the stationary solutions of Eq. (13) for α in two interesting cases: $\epsilon = 0.1$ where we predict the occurrence of a window with 3 stationary solutions, and $\epsilon = 0.5$ where one has a maximum of 2 stationary solutions satisfying the normalizability conditions $\tilde{\omega}_x^2 > 0$ and $\tilde{\omega}_y^2 > 0$. The dashed-dotted line corresponds to the stationary solution of the non interacting gas. In both Figs. 2 and 3 one identifies two branches, hereafter called normal and overcritical branches.

a. Normal branch: this branch starts at $\Omega = 0$. The linear dependence at small Ω is given by $\alpha = -\Omega\epsilon$. By increasing Ω the square radius $\langle y^2 \rangle$ increases and eventually diverges at $\Omega = \omega_y$ where $\tilde{\omega}_y \rightarrow 0$ and the branch has its end [15]. Also the angular momentum and the release energy diverge at $\Omega = \omega_y$. Notice that when $\tilde{\omega}_y \rightarrow 0$ the moment of inertia takes the rigid value since $\langle x^2 \rangle \ll \langle y^2 \rangle$ (see Eq.(11)).

b. Overcritical branch: this branch starts at $\Omega = +\infty$ where α behaves like $\alpha = (\omega_x^2 - \omega_y^2)/4\Omega$. It is worth noticing that in this limit both $\tilde{\omega}_x^2$ and $\tilde{\omega}_y^2$ approach the value $(\omega_x^2 + \omega_y^2)/2$ and therefore the shape of the density profile becomes symmetric despite the asymmetry of the confining trap. In the same limit the angular momentum tends to zero while the release energy approaches the finite value $E_{\text{rel}} = (2/7)\tilde{\mu}_\infty$, where $\tilde{\mu}_\infty$ is the chemical potential (8) with $\tilde{\omega}_x^2 = \tilde{\omega}_y^2 = (\omega_x^2 + \omega_y^2)/2$. In the overcritical branch the deformation of the cloud takes a sign opposite to the one of the trap. This branch exhibits a back-bending at a value of Ω which is smaller than ω_x , but can be higher or smaller than ω_y , depending on whether the value of ϵ is larger or smaller than 0.2 (see Figs. 2 and 3). In both cases this branch ends, after the back-bending, at the value $\Omega = \omega_x$, where $\tilde{\omega}_x \rightarrow 0$ and $\langle x^2 \rangle$, $\langle L_z \rangle$ and E_{rel} diverge.

It is also useful to discuss the instructive case $\epsilon \rightarrow 0$ corresponding to symmetric trapping in the x - y plane ($\omega_x = \omega_y$). In this case one finds a solution with $\alpha = 0$ for $\Omega < \omega_x/\sqrt{2}$ [16]. For higher frequencies three solutions appear: the first one still corresponds to a non-rotating configuration ($\alpha = 0$), while two solutions, given respectively by $\alpha = \pm \sqrt{2\Omega^2 - \omega_x^2}$, correspond to rotating deformed configurations. The existence of these solutions, which break the original symmetry of the Hamiltonian, is the analog of the bifurcation from the axisymmetric Maclaurin to the triaxial Jacobi ellipsoids for rotating classical fluids [17]. It is worth pointing out that the existence of the bifurcation is the consequence of two-body interactions and is absent in the non-interacting Bose gas. When ϵ is slightly different from zero (and positive) the two solutions are no longer degenerate, the one with $\alpha < 0$ having the lowest energy.

The existence of stationary solutions in the rotating frame raises the important question of stability. Actually, one should distinguish between thermodynamic and dynamical instability. The former corresponds to the absence of thermodynamic equilibrium and its signature, at zero temperature, is given by the existence of excitations with negative energy [16]. The latter is instead associated with the decay of the initial configuration due to interaction effects and is in general revealed by the appearance of excitations with complex energy. Configurations characterized by thermodynamic instability are destabilized only in the presence of dissipative processes.

Let us first discuss the stability with respect to the center of mass motion. In the presence of harmonic trapping the corresponding equations of motion, in the rotating frame, take the classical form (rotating Blackburn's pendulum,

[1]) and are not affected by interatomic forces. Their solutions obey the dispersion law

$$\omega^2 = \frac{1}{2} \left[\omega_x^2 + \omega_y^2 + 2\Omega^2 \pm \sqrt{(\omega_x^2 - \omega_y^2)^2 + 8\Omega^2(\omega_x^2 + \omega_y^2)} \right], \quad (16)$$

and are dynamically stable ($\omega^2 > 0$) for $\Omega < \omega_y$ and $\Omega > \omega_x$. So the requirement that the dipole oscillation be dynamically stable excludes the region between the dotted lines in Figs. 1, 2 and 3. Notice that this is the same region where the Schrodinger equation for the non-interacting Bose gas has no stationary solutions in the rotating frame.

We have further explored the conditions of stability by studying the quadrupole oscillations of the condensate around the equilibrium configuration in the rotating frame. The calculation is derivable by linearizing the equations of motion (1) and (2), with the choice

$$\delta\rho(\mathbf{r}) = a_0 + a_x x^2 + a_y y^2 + a_z z^2 + a_{xy} xy \quad (17)$$

$$\delta\mathbf{v}(\mathbf{r}) = \nabla(\alpha_x x^2 + \alpha_y y^2 + \alpha_z z^2 + \alpha_{xy} xy), \quad (18)$$

for the fluctuations of the density and of the velocity field where the coefficients a_i and α_i depend on time. The results of the analysis show that the window of dynamical instability for the quadrupole oscillations is different from the one of the dipole. In particular the normal branch is always dynamically stable, while the overcritical branch is stable only in its lower part since, after the back-bending, where $d\alpha/d\Omega > 0$, one of the quadrupole frequencies becomes purely imaginary ($\omega^2 < 0$). We have investigated the stability of the quadrupole excitations also in the limiting case $\epsilon = 0$. In this case the upper and lower branches $\alpha = \pm\sqrt{2\Omega^2 - \omega_x^2}$ give rise to a vanishing value for one of the quadrupole frequencies, the others being always real. This vanishing solution corresponds to the rotation of the system in the $x - y$ plane and reflects the rotational symmetry of the Hamiltonian.

We stress again that the solutions discussed in this paper correspond, in general, to metastable configurations. For example it is well known that vortical configurations can become energetically favorable for relatively small values of Ω . Also excitations with higher multipolarities can become energetically favorable for some values of the angular velocity [18]. In this work we assume that at very low temperature, where collisions are rare, the solutions (3)-(4) can survive, at least for useful time intervals, also in conditions of thermodynamic instability.

Let us finally briefly discuss the experimental possibility of realizing the rotations described above. The normal branch, characterized by the huge increase of the size in the y direction and of the release energy when $\Omega \rightarrow \omega_y$, could be in principle generated by an adiabatic increase of the angular velocity, starting from a cold condensate [13]. The transition from the normal to the overcritical branch cannot be instead realized in a continuous way and the only way to realize the exotic configurations of this branch is to engineer the proper conditions of dynamical equilibrium, by building up both the proper phase of the order parameter and the shape of the density profile.

We are indebted to S. Vitale for introducing us to the problem of the overcritical rotations. Fruitful discussions with E. Cornell, J. Dalibard, L. Pitaevskii and G. Shlyapnikov are also acknowledged. This work has been supported by the Ministero della Ricerca Scientifica e Tecnologica (MURST).

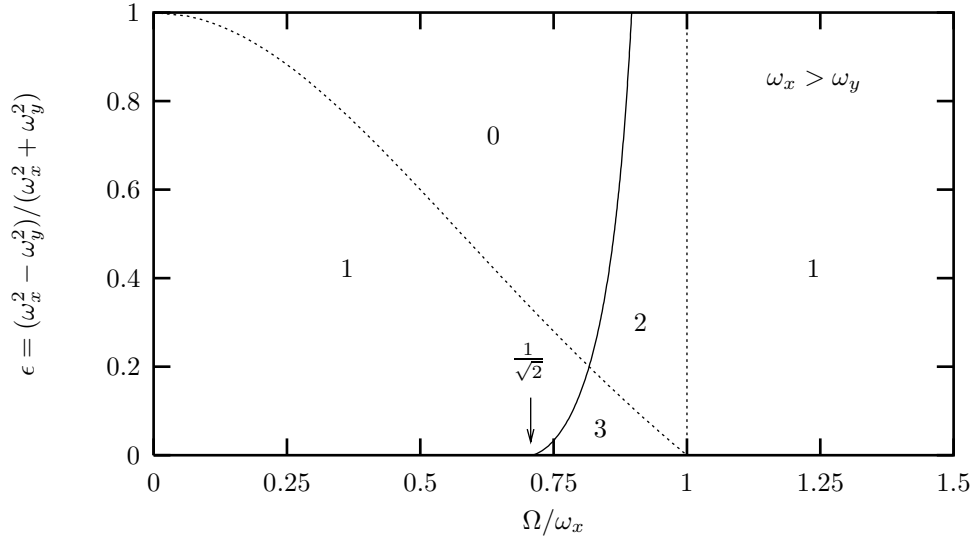


FIG. 1. Phase diagram representing the stationary solutions of Eq. (13) (see text). The dotted lines are the curves $\Omega = \omega_y$ and $\Omega = \omega_x$ respectively. The full line is given by Eq. (15).

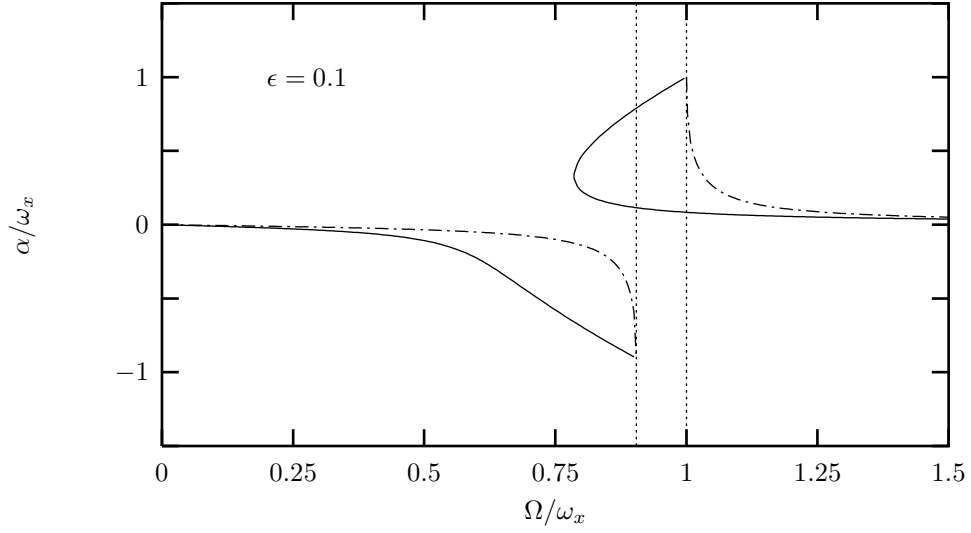


FIG. 2. Stationary solutions of Eq. (13) (solid lines) as a function of Ω , for $\epsilon = 0.1$. The dashed-dotted curves are the stationary solutions of the non-interacting Bose gas. The dotted straight lines correspond to $\Omega = \omega_y$ and $\Omega = \omega_x$ respectively.

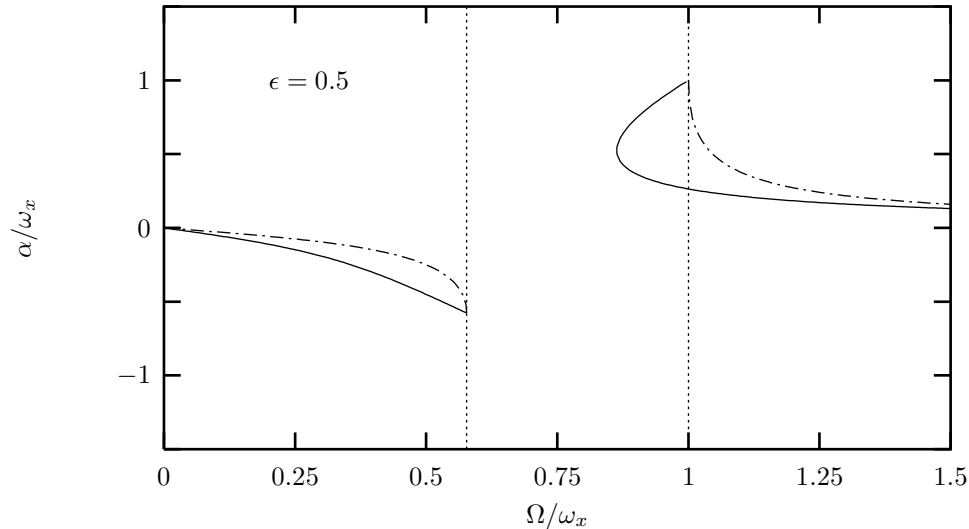


FIG. 3. As in Fig. 2, for $\epsilon = 0.5$.

-
- [1] H. Lamb, *Dynamics*, Cambridge University Press (2nd Ed.), 1923.
- [2] G. Genta, *Vibration of Structures and Machines*, Springer-Verlag, New York (third Ed), 1999.
- [3] R.J. Donnelly, *Quantized vortices in Helium II*, Cambridge University Press, Cambridge, 1995.
- [4] M.R. Matthews, B.P. Anderson, P.C. Haljan, D.S. Hall, C.E. Wieman, and E.A. Cornell, *Phys. Rev. Lett.* **83**, 2498 (1999).
- [5] K.W. Madison, F. Chevy, W. Wohlleben, and J. Dalibard, *Phys. Rev. Lett.* **84**, 806 (2000).
- [6] O.M. Maragò, S.A. Hopkins, J. Arlt, E. Hodby, G. Hechenblaikner, and C.J. Foot, *Phys. Rev. Lett.* **84**, 2056 (2000).
- [7] S. Stringari, *Phys. Rev. Lett.* **77**, 2360 (1996).
- [8] F. Dalfovo, S. Giorgini, L. Pitaevskii and S. Stringari, *Rev. Mod. Phys.* **71**, 463 (1999).
- [9] This choice, which is associated with a quadrupolar shape of the equilibrium density (see Eq. (4)), corresponds to one of the possible stationary solutions of the equations of motion.
- [10] L.P. Pitaevskii, *Sov. Phys. JETP* **13**, 451 (1961); E.P. Gross, *Nuovo Cimento* **20**, 454 (1961).
- [11] F. Dalfovo and S. Stringari, *Phys. Rev. A* **53**, 2477 (1996); E. Lundh, C.J. Pethick, and H. Smith, *Phys. Rev. A* **55**, 2126 (1997).
- [12] J.J. Garcia-Ripoll and V.M. Perez-Garcia, e-print cond-mat/0003451; F. Zambelli and S. Stringari, e-print cond-mat/0004325.
- [13] A. Recati, diploma thesis, Università di Trento (1999). Notice that this equation is independent of the equation of state $\mu_{loc}(\rho)$ entering Eq.(2) and holds, in particular, also for a trapped Fermi superfluid.
- [14] The value $\epsilon = 0.2$ corresponds to the intersection between Eq.(15) and the curve $\Omega = \omega_y$.
- [15] Near the end point the conditions of applicability of the Thomas-Fermi approximation are no longer valid and the solution of the problem should be obtained starting from the Gross-Pitaevskii equation.
- [16] The value $\Omega = \omega_x/\sqrt{2}$ corresponds to the value of the angular velocity for which the energy $\hbar\omega = \hbar(\sqrt{2}\omega_x - 2\Omega)$ of the $L_z = +2$ quadrupole oscillation, relative to an axisymmetric configuration, vanishes in the rotating frame [7]. For larger Ω the excitation energy becomes negative.
- [17] S. Chandrasekhar, *Ellipsoidal Figures at Equilibrium*, Yale University Press, 1969; P.G. Drazin, *Nonlinear Systems*, Cambridge University Press, Cambridge, 1994.
- [18] F. Dalfovo, S. Giorgini, M. Guilleumas, L. Pitaevskii, and S. Stringari, *Phys. Rev. A* **56**, 3840 (1997).